Supporting Information

Electronic structure tailored all non-precious Zn-promoted FeCo alloy anchored on porous N-doped carbon aerogel under thermal reduction for boosting oxygen evolution reaction

Yangxin Bai,‡[ab] Jiaxin Lu,‡[ab] Qi Yanli,[c] Yitian Shao,[ab] Ran Xie,[ab] Xiaodong Wu,*[abd] Xiaodong Shen,*[abd] Sheng Cui[abd] and Zhanwu Wu[e]

(a College of Materials Science and Engineering, Nanjing Tech University, Nanjing, 211816, China;

b Jiangsu Collaborative Innovation Center for Advanced Inorganic Function Composites, Nanjing Tech University, Nanjing, 211816, China;

c School of Materials Science and Engineering, Changzhou University, Changzhou 213164, People's Republic of China

d State Key Laboratory of Materials-Oriented Chemical Engineering, College of Materials Science and Engineering, Nanjing Tech University, Nanjing, 211816, China;

e Shanghai Space Propulsion Technology Research Institute, Huzhou 313000, China)

Corresponding author's Email: wuxiaodong@njtech.edu.cn.

‡ Yangxin Bai and Jiaxin Lu contributed equally to this study.

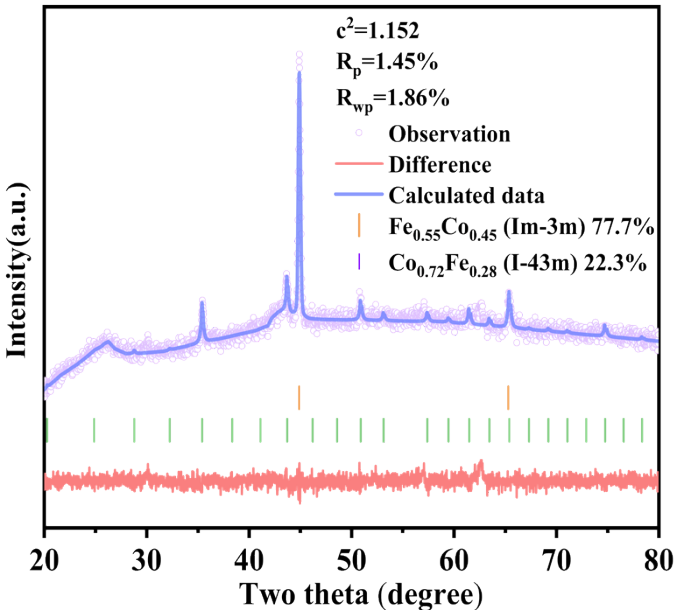

Fig. S1 Rietveld refinement on the XRD pattern of Zn-FeCo@NCA.

Table S1. Occupancy information for $Fe_{0.55}Co_{0.45}$-Im3m

Atom	Wyckoff	S.o.f.	x	y	z
Fe1	2a	0.550000	0.000000	0.000000	0.000000
Co1	2a	0.450000	0.000000	0.000000	0.000000

Table S2. Occupancy information for $Co_{0.72}Fe_{0.28}$-I43m

Atom	Wyckoff	S.o.f.	x	y	z
Fe1	2a	0.280000	0.000000	0.000000	0.000000
Fe2	8c	0.280000	0.320100	0.320100	0.320100
Fe3	24g	0.280000	0.359500	0.359500	0.042000
Fe4	24g	0.280000	0.092800	0.092800	0.280600
Co1	2a	0.720000	0.000000	0.000000	0.000000
Co2	8c	0.720000	0.320100	0.320100	0.320100
Co3	24g	0.720000	0.359500	0.359500	0.042000
Co4	24g	0.720000	0.092800	0.092800	0.280600

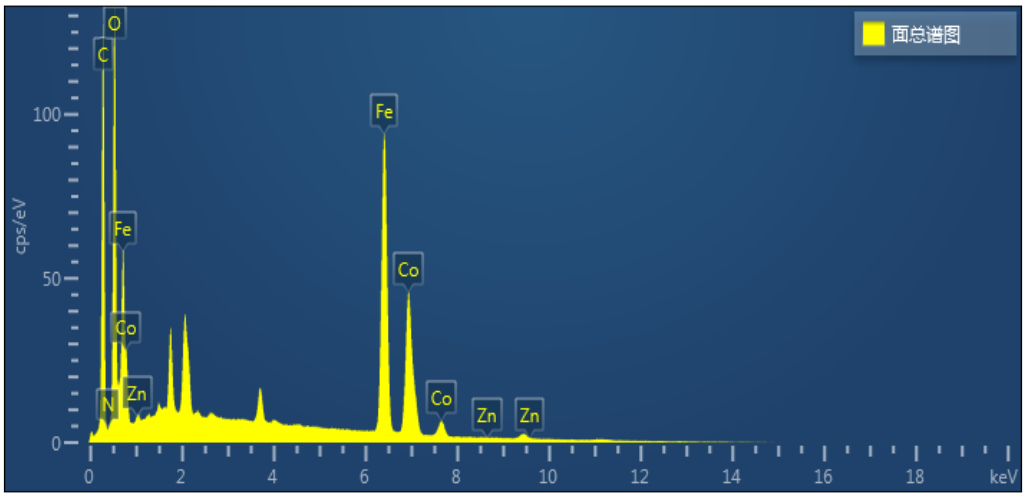

Fig. S2 EDS spectrum of the resulting Zn-FeCo@NCA sample.

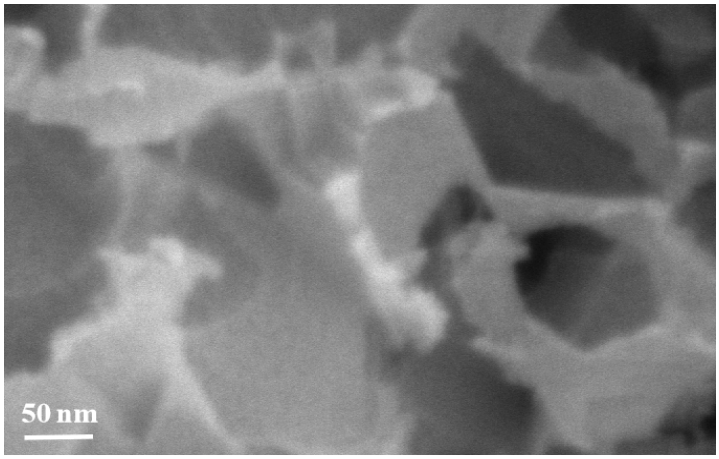

Fig. S3 SEM images of the NCA sample.

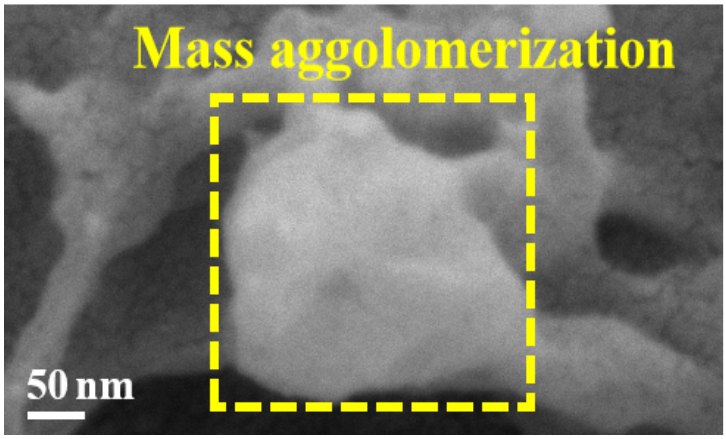

Fig. S4 SEM images of the FeCo@NCA sample.

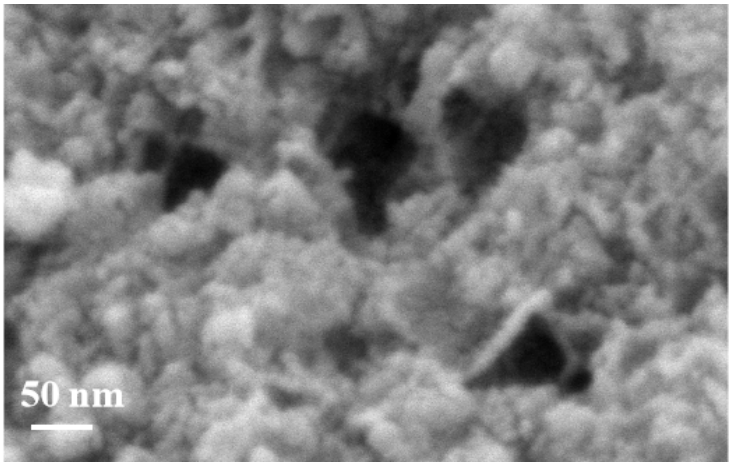

Fig. S5 SEM images of the Zn-FeCo@NCA sample.

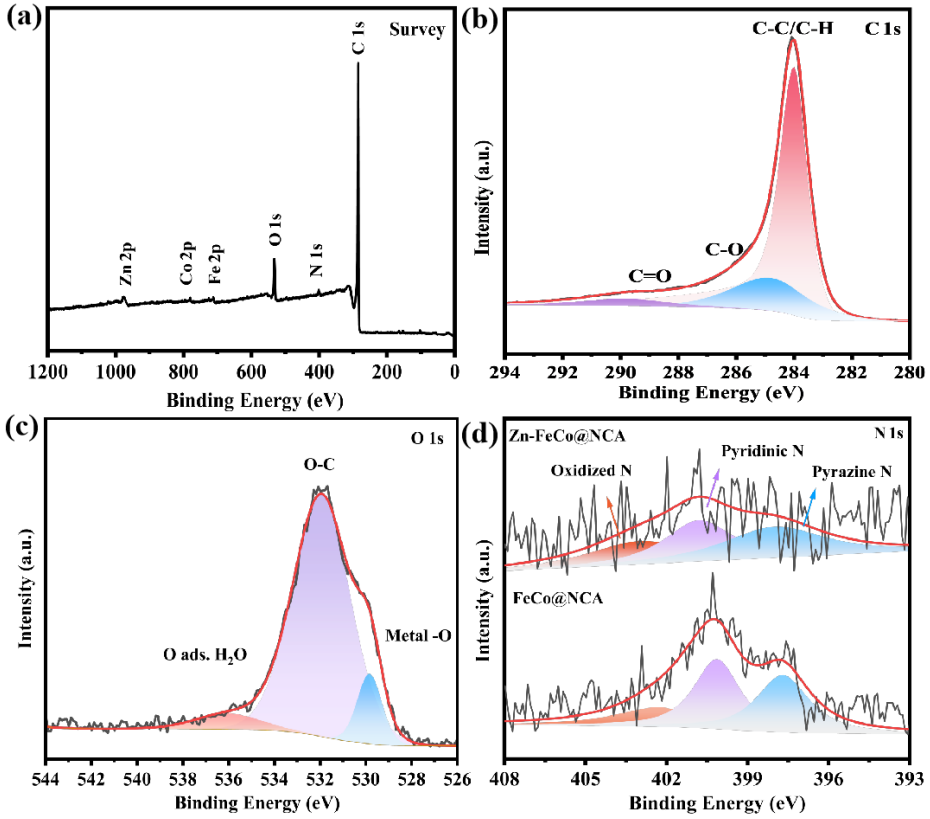

Fig. S6 (a) Full spectrum of XPS for the Zn-FeCo@NCA electrocatalyst; The high-resolution XPS spectra of (b) C 1s; (c) O 1s; and (f) N 1s for the resulting samples for comparison.

Table S3. Surface chemical compositions of the resulting samples were calculated by the Lorentzian-Gaussian function.

Samples	Fe 2p /binding	Energy /amount	Co2p /binding	Energy /amount	Zn 1s /binding	Energy /amount
Zn-FeCo@NCA	Fe^0 $2p^{3/2}$	707.2 5.0%	Co^0 $2p^{3/2}$	778.5 13.4 %	Zn^0 $2p^{3/2}$	1021.5 62.48%
	Fe^{2+} $2p^{3/2}$	710.2 63.3%	Co^{2+} $2p^{3/2}$	526780.2 56.2%	Zn^0 $2p^{1/2}$	1044.8 37.52%
	Fe^{2+} $2p^{1/2}$	723.4 31.6%	Co^0 $2p^{1/2}$	777.9 8.9%	/	/
			Co^{2+} $2p^{1/2}$	780.0 28.1%	/	/
FeCo@NCA	Fe^0 $2p^{3/2}$	706.7 7.5%	Co^0 $2p^{3/2}$	779.3 15.2%	/	/
	Fe^{2+} $2p^{3/2}$	710.1 61.7%.	Co^{2+} $2p^{3/2}$	781.8 53.7%	/	/
	Fe^{2+} $2p^{1/2}$	723.1 30.8%	Co^0 $2p^{1/2}$	796.0 8.3%	/	/
			Co^{2+} $2p^{1/2}$	795.8 22.8%	/	/

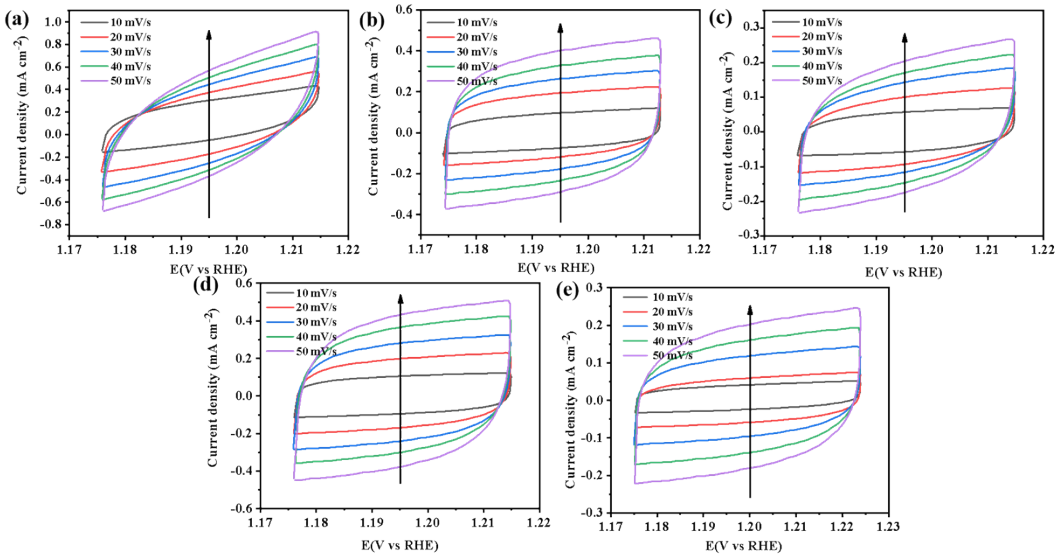

Fig. S7 CV curves of (a) $Zn_{0.1}$-FeCo@NCA; (b) $Zn_{0.5}$-FeCo@NCA; (c) Zn_1-FeCo@NCA; (d) FeCo@NCA; and (e) RuO_2 at different scan rates.

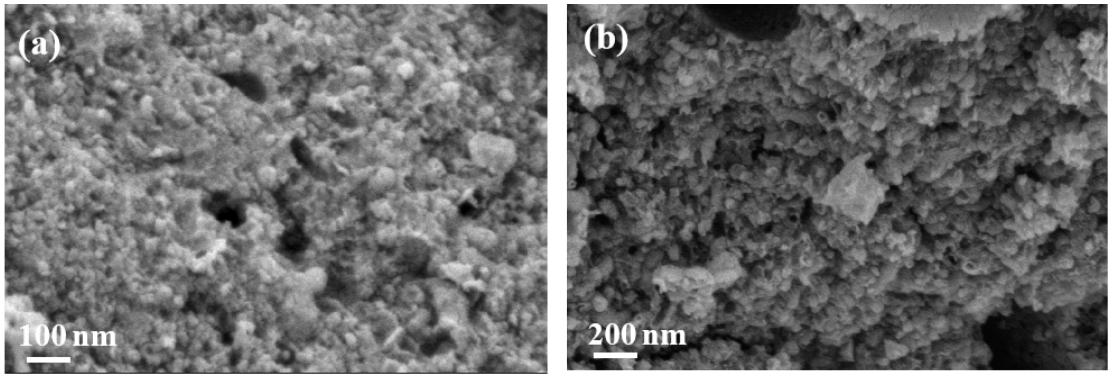

Fig. S8 SEM images of $Zn_{0.5}$-FeCo@NCA aerogel after potentiostatic polarization test.

Table S4. Comparison of OER performance of as-prepared $Zn_{0.5}$-FeCo@NCA and other similar electrocatalysts reported in the literature.

Sample	Overpotential (mV)	Tafel slope ($mV \cdot dec^{-1}$)	Reference
$Zn_{0.5}$-FeCo@NCA	270	75.5	This work
$LaNi_{0.7}$ $Fe_{0.25}O_3$	320	79.9	[1]
$CoSe_2$/Co	318	91.11	[2]
FeCo/CNF	490	102.5	[3]
$RuNi_7FeO_x(OH)_y$@NCA	278	102.7	[4]
(FeCoNiCuZn)O	323	64.5	[5]
CoCuFe	338	117.5	[6]
Co_3O_4@rGO	380	153	[7]
5% Ce-doped LDH	340	130	[8]
$Co(OH)_2$NF	396	112	[9]
NSCA/FeCo	355	60	[10]
CoOOH-Cs^+	355	66	[11]
Fe-CoOOH/G	330	93	[12]
$Co_{0.89}Ca_{0.11}$-CPs	371	58.3	[13]
Co/Mo-rGO	420	169	[14]

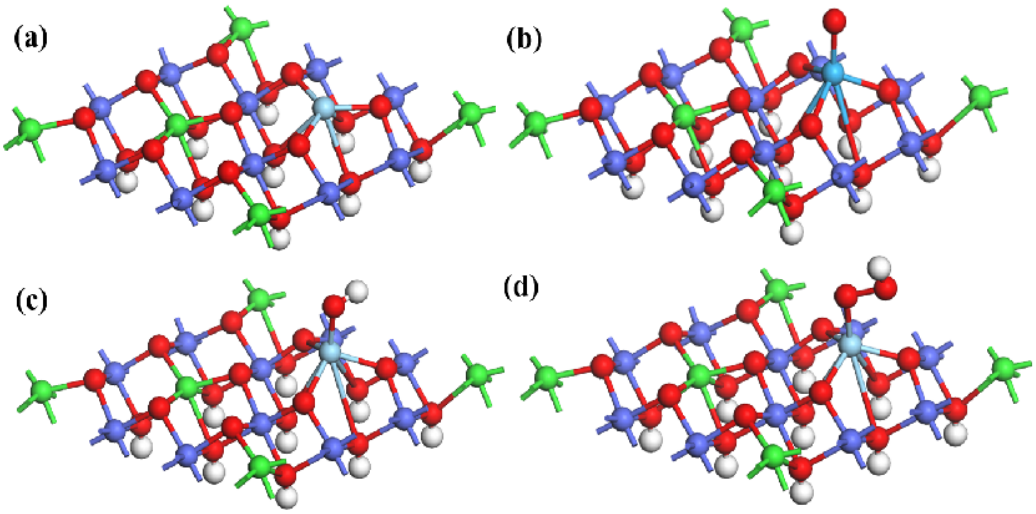

Fig. S9 Optimized configureurations of the (a) *; (b) *OH; (c) *O; and (d) *OOH adsorbed on the active Zn for the Zn-FeCo@NCA sample (the white, red, green, deep blue, and pale blue atoms represent the H, O, Fe, Co, and Zn atoms).

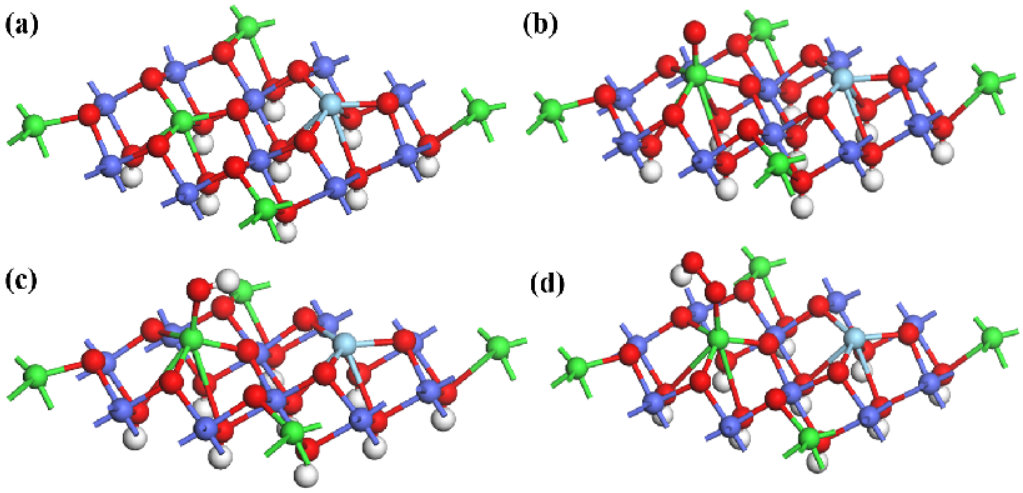

Fig. S10 Optimized configureurations of the (a) *; (b) *OH; (c) *O; and (d) *OOH adsorbed on the active Fe for the Zn-FeCo@NCA sample.

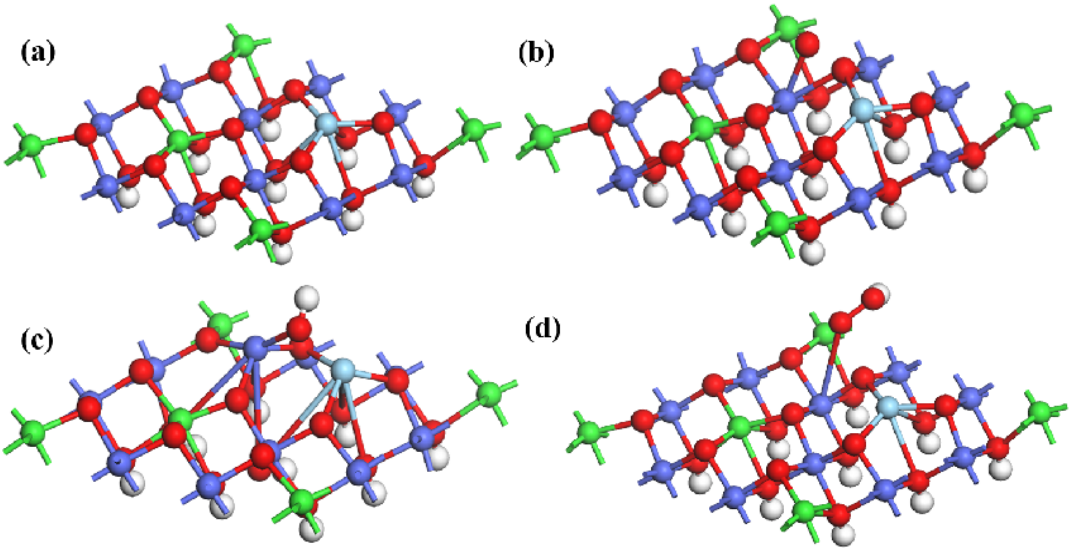

Fig. S11 Optimized configureurations of the (a) *; (b) *OH; (c) *O; and (d) *OOH adsorbed on the active Co for the Zn-FeCo@NCA sample.

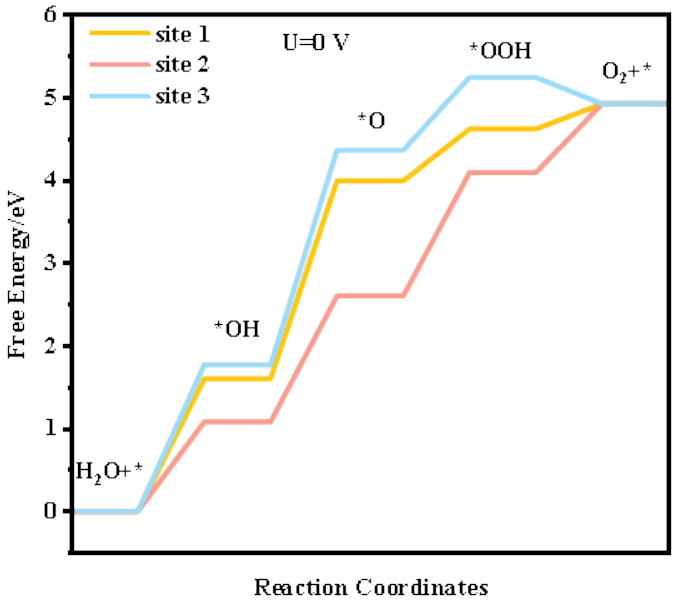

Fig. S12 The DFT calculations for the Gibbs free energy curves of the four OER elementary steps at U=0 V.

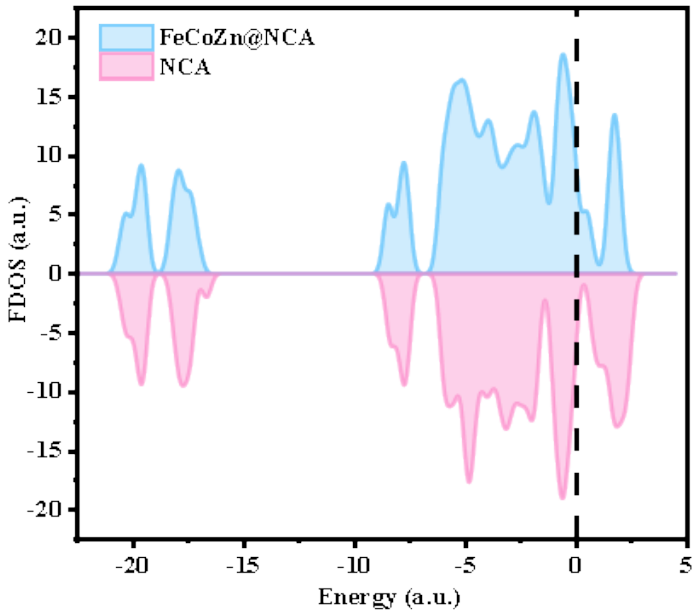

Fig. S13 FDOS of O of the resulting Zn-FeCo@NCA sample.

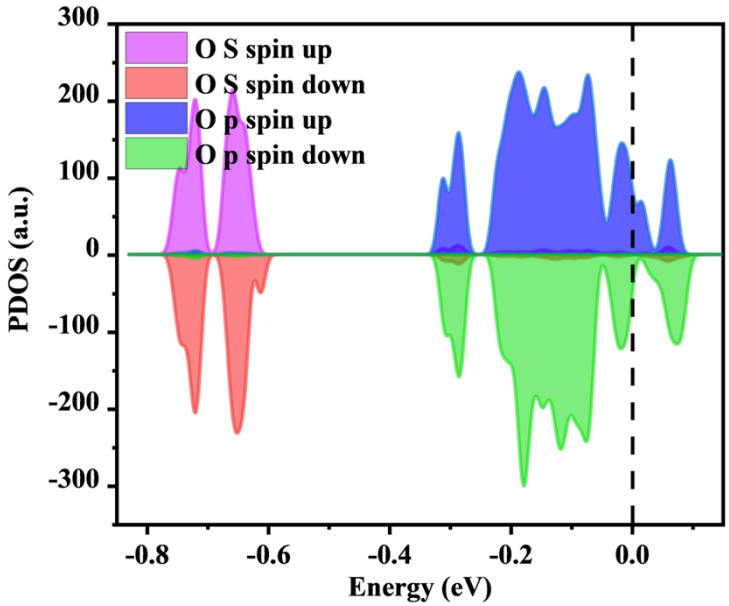

Fig. S14 PDOS of O of the resulting Zn-FeCo@NCA sample.

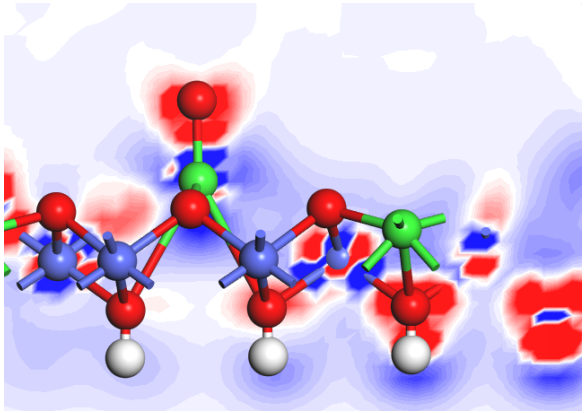

Fig. S15 The electron density slice of the optimized configurations of the Zn-FeCo@NCA (red for large value, blue for small value).

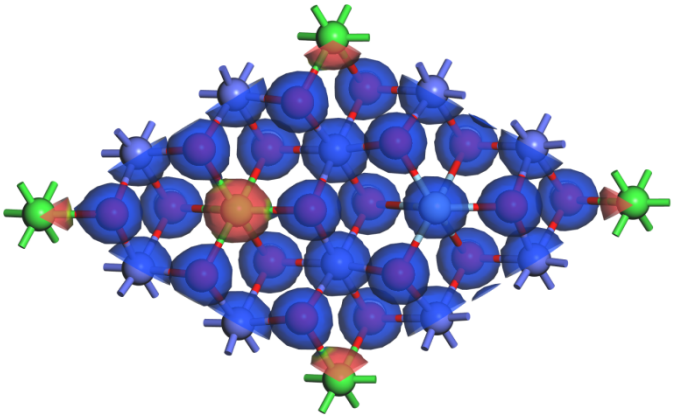

Fig. S16 The spin-electron density of optimized configurations of the Zn-FeCo@NCA (red for large value, blue for small value).

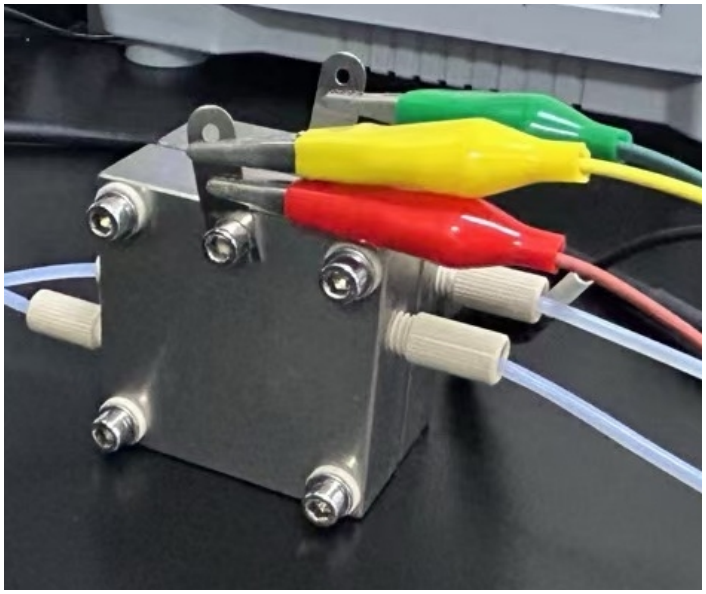

Fig. S17 A digital photograph of the operating AEMWE.

Table S5**.** Fitting results of the XPS spectra of the initial $Zn_{0.5}$-FeCo@NCA and $Zn_{0.5}$-FeCo@NCA after the OER test

Sample codes		Initial $Zn_{0.5}$-FeCo@NCA		$Zn_{0.5}$-FeCo@NCA after OER test	
Regions	Bonds	B. E. (eV)	Amount	B. E. (eV)	Amount
Fe $2p_{1/2}$	Fe^{2+}	723.7	22.32 %	/	/
	Fe^{3+}	726.0	12.58 %	721.2	34.64 %
Fe $2p_{3/2}$	Fe^{2+}	710.2	39.35 %	/	/
	Fe^{3+}	712.7	25.75 %	710.2	65.36 %
Co $2p_{3/2}$	Co^{2+}	779.7	46.24 %	779.7	8.97 %
	Co^{3+}	782.3	43.98 %	781.4	57.76 %
Co $2p_{1/2}$	Co^{2+}	794.5	18.57 %	794.2	4.58 %
	Co^{3+}	796.1	6.22 %	796.5	28.70 %

References

[1] J. Zhang, Y. Ye, B. Wei, F. Hu, L. T. Sui, H. W. Xiao, L. Q. Gui, J. Sun, B. B. He, and L. Zhao, *Appl. Catal. B,* **2023,** 330,122661.

[2] K. Zhao, X. Chen, H. Liu, J. Wang, and J. Zhang, *ACS Appl. Nano Mater.,* 2024, **7**, 6927-6934.

[3] L. Sun, M. Feng, Y. Peng, X. Zhao, Y. Shao, X. Yue, and S. Huang, *J. Mater. Chem. A* 2024, **12**, 8796-8804.

[4] S. Huang, J. Lu, X. Wu, H. Zhu, X. Shen, S. Cui, amd X. Chen, *Appl. Catal. A: Gen.,* 2023, **664**, 119331.

[5] Y. Lao, X. Huang, L. Liu, X. Mo, J. Huang, Y. Qin, Q. Mo, X. Hui, Z. Yang, and W. Jiang, *Chem. Eng. J.,* 2024, **481**, 148428.

[6] J. J Feng, J. T. Liu, C. H. Chu, L. L. Wei, H. Y. Li, and J. Q. Shen, *Chem. Eng. J., 2024,* **486**, 150359.

[7] R. Santhosh Kumar, S. C. Karthikeyan, S. Ramakrishnan, S. Vijayapradeep, A. Rhan Kim, J. S. Kim, and D. Jin Yoo, *Chem. Eng. J.,* 2023, **451**, 138471.

[8] M. Zubair, P. Kumar, M. Klingenhof, B. Subhash, J. A. Yuwono, S. S. Cheong, Y. Yao, L. Thomsen, P. Strasser, R. D. Tilley, and N. M. Bedford, *Acs Catal.,* 2023, **13,** 4799-4810.

[9] K. Y. Zhao, Y. Tao, L. K. Fu, C. Li, B. and J. Xu, *Chem. Int. Edit.,* 2023, **62**, e202308335.

[10] Y. Zhang, X. Zhang, Y. Li, J. Wang, S. Kawi, and Q. Zhong, *Nano Res.,* 2023, **16**, 6870-6880.

[11] H. N. Jia, N. Yao, C. Yu, H.J. Cong, and W. Luo, *Angew. Chem. Int. Edit.* 2023, **62**, e202313886.

[12] X. Han, C. Yu, S. Zhou, C. Zhao, H. Huang, J. Yang, Z. Liu, J. Zhao, and J. Qiu, Adv. Energy Mater., 2017, **7**, 1602148.

[13] P. P. Su, S. S. Ma, W. J. Huang, Y. Boyjoo, S. Y. Bai, and J. Liu, *J. Mater. Chem. A* 2019, 7 (2019) 19415-19422.

[14] L. Zhao, S. Liu, L. Wei, H. He, B. Jiang, Z. Zhan, J. Wang, X. Li, and W. Gou, Catalysis Letters, 2024, **154**, 5294-5302.